Determination of third-order nonlinear optical susceptibilities of polysilane thin films

C. L. Callender, C. A. Carere, and J. Albert

Communications Research Centre, P.O. Box 11490, Station H, Ottawa, Ontario K2H 8S2, Canada

L.-L. Zhou and D. J. Worsfold

Institute for Environmental Chemistry, National Research Council, Ottawa, Ontario K1A 0R9, Canada

Received June 10, 1991; revised manuscript received September 23, 1991

Third-order nonlinear optical susceptibilities $\chi^{(3)}(-3\omega;\omega,\omega,\omega)$ have been measured by third-harmonic generation for thin films of a series of polysilane polymers and copolymers and polycarbosilanes with different alkyl and aryl side groups. $\chi^{(3)}(-3\omega;\omega,\omega,\omega)$ values for all the polymers studied were found to be in the range 0.3×10^{-12}–4.5×10^{-12} esu. Factors affecting the magnitude of $\chi^{(3)}$, including the nature of the substituents, Si sequence length, polymer conformation, and film preparation, are discussed.

INTRODUCTION

Third-order nonlinearities in organic materials have attracted considerable interest recently owing to their potential applications in optical switching and optical computing devices.[1,2] Organic materials offer many advantages over the inorganic materials developed to date, including large nonlinearities with fast response times and ease of processing. However, π-conjugated carbon-based polymers, which so far have proved to be the most promising candidates for third-order nonlinear materials, often suffer the disadvantages of having large absorption bands in the visible or near-infrared regions of the spectrum and chemical instability.

Polysilanes are a distinct class of polymer that offer physical, chemical, and optical properties that render them suitable for various applications in optics. Linear polysilanes are thermally and oxidatively stable polymers that consist of a Si backbone with two side groups attached to each Si atom. They are transparent throughout the visible and near-infrared regions but exhibit large absorption bands in the 250–400-nm region, depending on the substituents, Si repeat length, crystallinity, and orientation. Polysilanes have been developed as photoresists for e-beam lithography[3] and ultraviolet photolithography,[4–6] and exploitation of the birefringence produced following two-photon absorption of visible light[7,8] allows for the fabrication of optical device structures such as channel waveguides and gratings.[9,10] Previously, some substituted polysilanes were shown to have $\chi^{(3)}$ coefficients in the range 10^{-12}–10^{-11} esu.[11–14] Although these values are not as large as those of other organic materials, e.g., polydiacetylenes,[15] the effects of substituent groups and orientation effects in polysilanes on the nonlinear optical properties have not yet been fully investigated, and further increases in $\chi^{(3)}$ may be possible through appropriate selection of side groups. The major advantage of a broad range of optical transparency makes further investigation of these materials highly desirable.

In this paper we present measurements of $\chi^{(3)}(-3\omega;\omega,\omega,\omega)$ by third-harmonic generation (THG) on a series of substituted polysilanes. For comparison, values were also measured for two polycarbosilanes, which contain short Si sequences interrupted by carbon backbone sequences. This study is part of an effort to identify promising new materials for applications in nonlinear optical devices.

EXPERIMENTAL TECHNIQUES

Polysilanes were synthesized by coupling the appropriate dichlorosilanes with the use of metallic Na dispersed in refluxing toluene (Wurtz synthesis) as described previously.[16] The random copolymer was prepared by polymerizing a mixed silane feed, whereas the block copolymer was prepared by reacting one monomer completely and then adding the second silane. Low molecular weight polysilane (<3000 molecular weight) was isopropanol soluble and was removed during workup. The normal Wurtz synthesis gave a polymer with a bimodal molecular weight distribution. Some polymerizations were carried out in the presence of a crown ether (1,4,7,10,13-pentaoxacyclopentadecane) to give a single molecular weight maximum. Polycarbosilanes were synthesized by coupling the appropriate dichlorosilanes and α,α'-dichloroxylene in a procedure similar to that described for the polysilanes.

Molecular weights of polysilanes and polycarbosilanes were determined by gel permeation chromatography in tetrahydrofuran, with the use of both refractive index and ultraviolet absorbance detectors. Elution volumes were converted to molecular weights by a comparison with polystyrene standards. This method does not give absolute molecular weights because of differing hydrodynamic behavior but is reliable to within 50%; within the respective polymer series (polysilanes and polycarbosilanes), relative molecular weights are reliable to within 10%. Polymer structures and molecular weights are collected in Table 1.

0740-3224/92/040518-06$05.00

Table 1. Structures, Molecular Weights, and Absorption Maxima for Polysilanes and Polycarbosilanes

	Polymer Structure	Peak Molecular Weight[a]	λ_{max} (nm)
A	$(PhSiMe)_n$	1.0×10^4	332
B	$(c\text{-HexylSiMe})_n$	2.5×10^5 1.0×10^4 Bimodal	314
C	$(n\text{-PropylSiMe})_n$	5.0×10^4	322
D	(PhSiMe)(MeSiMe) Random copolymer	1.0×10^4	322
E	$(PhSiMe)_m(n\text{-hexylSiMe})_n$ Block copolymer	4.0×10^5 5.0×10^3 Bimodal	332
F	$[(MeSiMe)_4(CH_2\text{–}Ph\text{–}CH_2)]_n$ Random polycarbosilane	2.0×10^3	295
G	$[(n\text{-HexylSiMe})_8(CH_2\text{—}Ph\text{—}CH_2)_2]_n$ Random polycarbosilane	1.1×10^2	291

[a] By gel permeation chromatography, relative to polystyrene standards.

Thin films were deposited by spinning solutions of each polymer in toluene onto 1.25-in. (3.18-cm) -diameter Si wafers and 1-in.-diameter by 0.625-in.-thick fused-silica flats. Substrates were cleaned by consecutive immersion in hot hydrogen peroxide–ammonium hydroxide and hydrogen peroxide–hydrochloric acid mixtures, followed by copious rinsing with pure water. Surfaces were prepared for spinning by immersion of substrates in a 2% v/v solution of dimethyldichlorosilane in distilled chloroform. Concentrations of polymer solutions were typically 50–150 mg/mL. The solutions were filtered through a 0.45-μm MF-Millipore filter, deposited onto substrates from a syringe, and spun at 3000 rpm for 15 s. The resulting films had thicknesses in the range 80–600 nm. Films were dried for a few hours under vacuum and protected from daylight. Thicknesses and refractive indices were determined for films deposited onto Si wafers with an Applied Materials ellipsometer operating at 546 nm. The correct number of thickness multiples determined by ellipsometry was confirmed for films on fused silica by a Tencor Instruments Alpha-Step profiler (for films thicker than 400 nm) or by a Leitz optical microscope with a Michelson interferometer attachment. Ultraviolet–visible absorption spectra of films of varying thicknesses were obtained with a Cary 3 spectrophotometer and provided a further confirmation of film thicknesses. All the polysilanes exhibited a large absorption band in the 250–350-nm region (see, for example, Fig. 1). The absorption maximum for each polysilane (in the form of a film) is listed in Table 1. The absorbance at 355 nm in each case was close to zero. Thicknesses determined from absorbance measurements were in good agreement with those determined by ellipsometry; values obtained from these two methods were used for all the calculations.

THG measurements were carried out with a pulsed Q-switched Nd:YAG laser operating at 1064 nm with a repetition rate of 10 Hz and a pulse width of 10 ns. For a pulse energy of 0.5–0.7 mJ, the beam was focused with a 30-cm lens, and the sample was located approximately 0.5 cm from the focus. This arrangement gave power densities of ~200 MW cm^{-2} at the sample. All the films supported these power densities without signs of damage. The samples (polymer films on fused-silica substrates) were held vertically with the film toward the detector and were mounted on a rotation stage. Although it is desirable to house the sample and the stage in a vacuum chamber, this facility was not readily available. A vacuum chamber is currently under construction for future experiments. Maker fringes were generated by rotating the sample through the range −30° to +30° from normal. The polarization of the laser beam was maintained parallel to the rotation axis by means of a quarter-wave plate–polarizer combination. The third-harmonic radiation at 355 nm was detected by a Hamamatsu R943-02 photomultiplier. A series of filters was mounted in front of the detector to cut out the incident pump wavelength (two Corning 7-54 glass filters, one Hoya U340 glass filter, and an ARC 355-nm bandpass filter). Data were collected with the use of an EG&G PARC 162 boxcar averager and a Keithley 199 digital multimeter. Rotation of the sample stage and data collection were controlled by a personal computer. The experimental arrangement is shown in Fig. 2.

DATA ANALYSIS

Maker fringes (oscillations in intensity) are observed in optical THG from multilayer structures as the sample is rotated in the plane containing the incident pump beam. They are due to interference between harmonic free and bound waves generated in the various layers, coupled to the dispersion in phase velocity between the pump and harmonic waves. Our analysis to obtain the third-order nonlinear susceptibility $\chi^{(3)}(-3\omega;\omega,\omega,\omega)$ from the fringe measurements is similar to the one presented in Ref. 17. Throughout the following discussion the third-order susceptibility will be abbreviated as $\chi^{(3)}$. In this study we found it unnecessary to use complex $\chi^{(3)}$ values to obtain a good fit to the data. This correlates well with other polysilane results,[11,12,14] which showed small values for the phase of $\chi^{(3)}$ in similar experiments.

Assuming that there is no pump depletion, the total harmonic signal in our experimental configuration comes from four sources: substrate, thin film, and air on the two sides of the sample. We add the amplitudes of these signals at the detector, which was located far enough from

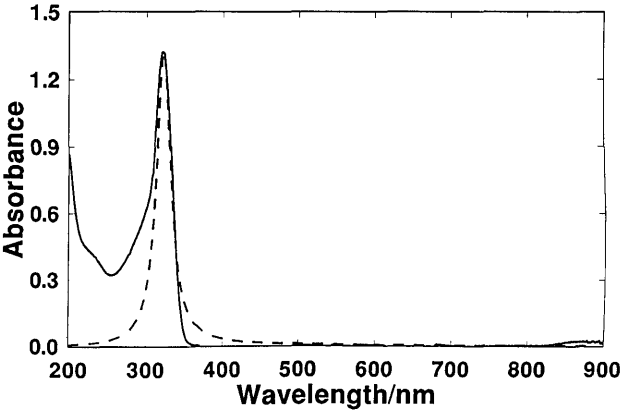

Fig. 1. Absorption spectrum of polysilane C, poly(methyl-n-propylsilane) (solid curve) with Kramers–Kronig fit (dashed curve) used to evaluate the refractive index at 355 nm.

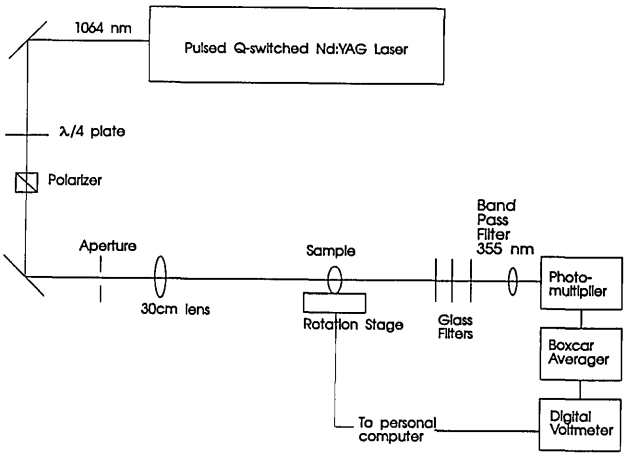

Fig. 2. Experimental arrangement for the measurement of THG from polysilane thin films.

the sample for air contributions in the diverging pump beam to have ended. Each signal accumulates phase shifts and amplitude transmission factors as it goes through the sample. Preliminary measurements on bare substrates indicated that the air contribution could not be neglected in our experimental configuration.

Taking the origin of the phase of all the waves to be the first interface between air and the substrate, the four contributions are as follows:

(1) Air contribution from the converging pump beam before the substrate:

$$E_{\mathrm{THG}} = C\exp\{i[\psi_{3s}(\theta) + \psi_{3f}(\theta)]\} \times T_{as}(3\omega,\theta)T_{sf}(3\omega,\theta)T_{fa}(3\omega,\theta)E_i^3/4 = A_1\exp[i(\psi_{3s} + \psi_{3f})], \quad (1)$$

where

C is a factor dependent on the nonlinear susceptibility and dispersion of air as well as on the geometry of the experiment;

$\psi_{3\alpha} = 3(2\pi/\lambda)n_\alpha(3\omega)l_\alpha\cos[\theta(3\omega,\alpha)]$ is the accumulated phase of the harmonic wave through medium α [where α stands for f (film) or s (substrate)];

$\theta(3\omega,\alpha)$ is the angle of the beam at 3ω through medium α;

$n_\alpha(3\omega)$ is the refractive index of medium α at frequency 3ω;

l_α is the thickness of medium α;

$T_{\alpha\beta}$ are the Fresnel electric field amplitude transmission coefficients between media α and β; and

E_i is the amplitude of the electric field of the incident pump wave.

Note that ψ and T depend on the angle of incidence.

(2) Contribution from the substrate:

$$E_{\mathrm{THG}} = \frac{\chi_s^{(3)}}{\Delta n_s{}^2}T_{as}{}^3(\omega,\theta)\{\exp[i\psi_{1s}(\theta)] - \exp[i\psi_{3s}(\theta)]\} \times \exp[i\psi_{3f}(\theta)]F_{sf}(\theta)T_{fa}(3\omega,\theta)E_i^3/4 = A_2[\exp(i\psi_{1s}) - \exp(i\psi_{3s})]\exp(i\psi_{3f}), \quad (2)$$

where

$\psi_{1\alpha} = 3(2\pi/\lambda)n_\alpha(\omega)l_\alpha\cos[\theta(\omega,\alpha)]$ is the accumulated phase of the cube of the pump wave;

$\chi_s^{(3)}$ is the third-order nonlinear susceptibility of the substrate;

$\Delta n_\alpha{}^2$ is the difference in the squares of the refractive indices at the fundamental and third-harmonic frequencies; and

$$F_{\alpha\beta} = \frac{n_\alpha(3\omega)\cos[\theta(3\omega,\alpha)] + n_\alpha(\omega)\cos[\theta(\omega,\alpha)]}{n_\alpha(3\omega)\cos[\theta(3\omega,\alpha)] + n_\beta(3\omega)\cos[\theta(3\omega,\beta)]}$$

is a factor arising from the boundary conditions.

(3) Contribution from the film:

$$E_{\mathrm{THG}} = \frac{\chi_f^{(3)}}{\Delta n_f{}^2}T_{as}{}^3(\omega,\theta)T_{sf}{}^3(\omega,\theta)\exp[i\psi_{1s}(\theta)]\{\exp[i\psi_{1f}(\theta)] - \exp[i\psi_{3f}(\theta)]\}F_{fa}(\theta)E_i{}^3/4 = A_3\exp(i\psi_{1s})[\exp(i\psi_{1f}) - \exp(i\psi_{3f})], \quad (3)$$

where $\chi_f^{(3)}$ is the third-order nonlinear susceptibility of the film.

(4) Air contribution from the diverging pump beam after the film:

$$E_{\mathrm{THG}} = -CT_{as}{}^3(\omega,\theta)T_{sf}{}^3(\omega,\theta)T_{fa}{}^3(\omega,\theta)\exp[i(\psi_{1s} + \psi_{1f})]E_i{}^3/4 = A_4\exp[i(\psi_{1s} + \psi_{1f})], \quad (4)$$

where the amplitude is taken as the negative of that of contribution (1), which implies that the focus is situated near the center of the sample. This is a valid approximation in our case because a weakly focusing lens was used. The contributions on both sides of the sample build up over several centimeters and are almost equal in spite of the 5-mm asymmetry.

Summing the four amplitudes and calculating the intensity yield the signal at the detector in the following form:

$$\begin{aligned} I_{\mathrm{THG}} = 2\{&[A_2{}^2 - A_2A_3 - A_2A_1 + A_3A_4 \\ &+ A_3{}^2 + (A_1{}^2 + A_4{}^2)/2] \\ &+ \cos(\Delta\psi_s)(A_2A_3 + A_2A_1 - A_2{}^2 - A_3A_1) \\ &+ \cos(\Delta\psi_f)(A_2A_3 + A_2A_4 - A_3{}^2 - A_3A_4) \\ &+ \cos(\Delta\psi_s + \Delta\psi_f)(A_1A_4 - A_2A_3 \\ &+ A_3A_1 - A_2A_4)\}, \end{aligned} \quad (5)$$

where $\Delta\psi_\alpha = \psi_{1\alpha} - \psi_{3\alpha}$.

To calculate the phases $\psi_{m\alpha}$ and the transmission factors $T_{\alpha\beta}$, we require the refractive indices of the media at both the pump and signal wavelengths. Along with the susceptibilities of the film and the substrate and the C parameter, there are a total of seven unknowns in Eq. (5) (assuming that the thicknesses of the film and the substrate are known).

Refractive index and susceptibility data for the substrates (fused silica) may be found in the literature. In fact, the refractive index dispersion can be checked easily from fringes obtained with a bare substrate [see Fig. 3(a)], with a precision limited only by the thickness measurement. We used $n_g{}^2(\omega) = 2.10$, $n_g{}^2(3\omega) = 2.176$, and $\chi_g^{(3)} = 3.11 \times 10^{-14}$ esu at 1064 nm.[17,18]

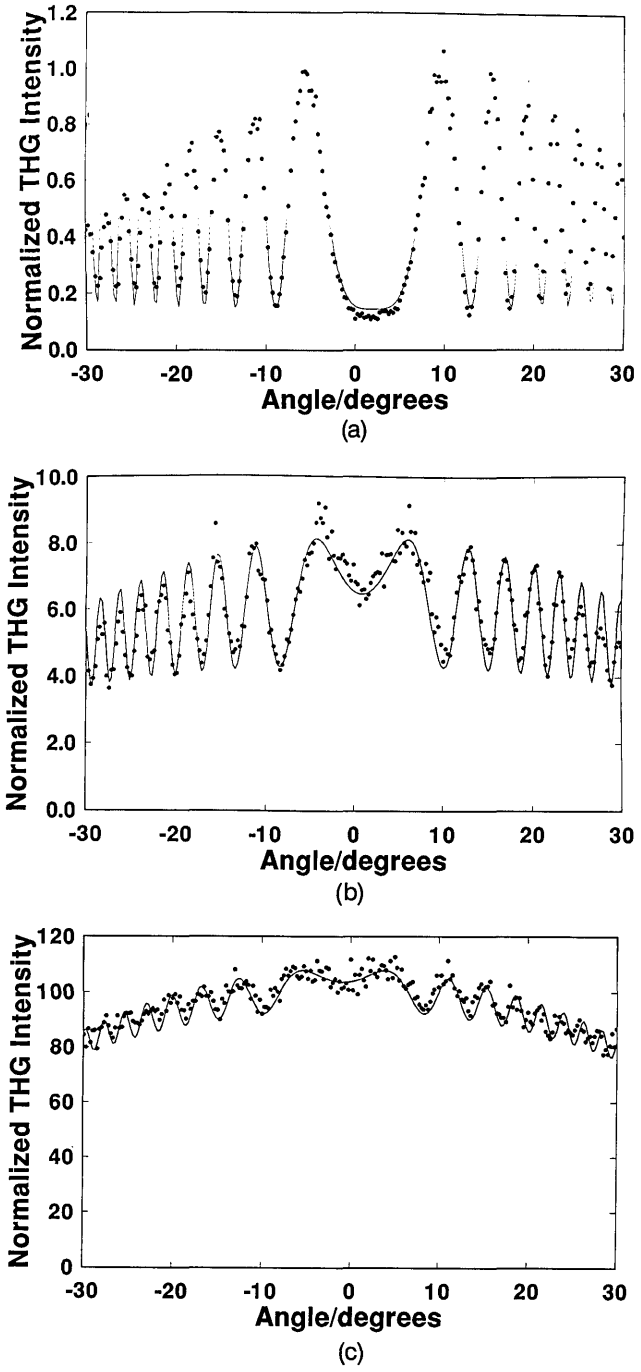

Fig. 3. Maker fringes generated in THG measurements (dots) and best fits to the data (solid curves) for (a) a bare fused-silica substrate, 1.63 mm thick, (b) a 227-nm-thick film of polysilane C [poly(methyl-*n*-propylsilane)], and (c) a 240-nm-thick film of polysilane D (methylphenylsilane–dimethylsilane random copolymer).

An ellipsometric measurement was used to determine the refractive index of the polysilanes at 546 nm. It was assumed that the transparency range extended beyond 1064 nm, and a Kramers–Kronig analysis indicated that the dispersion over the range 546–1064 nm is within the error limits of our ellipsometric measurements (±0.02). The refractive index at the third harmonic (355 nm) was obtained by fitting the ultraviolet absorption data with a Lorentzian oscillator and using a Kramers–Kronig analysis to calculate the index dispersion across this region of the spectrum. Figure 1 shows the fit to the absorption spectrum for a typical case. In all the cases the absorption at 355 nm was close to zero, and complex refractive index values were not required. Fits were carried out for two absorption peaks in appropriate cases, but this was found to yield the same result within error as a fit to only the lowest energy absorption band. Resultant values of the refractive indices at 546 nm (assumed to be close to the value at 1064 nm) and 355 nm are presented in Table 2. The uncertainties in the n(355 nm) values from the Kramers–Kronig fits were estimated to be ±10%, while the values of n(1064 nm) are accurate to ±2%. The ellipsometer measurement also yielded the thickness of the polysilane thin films to within ±2%.

The effect of the air parameter C may be divided into three different regimes. If the air contribution is of the same order of magnitude as contributions from the sample, interference occurs. The signal decreases overall, and the envelope of fringes acquires a complex shape. The other regimes occur when the air contribution is much smaller than that of the sample and therefore has little effect on the result and when the air contribution is much bigger than that of the sample. In the former case the fringes have maxima with almost-equal amplitudes and near-zero minima. In the latter case fringes result simply from the interference between waves generated in air before and after the sample and look remarkably similar to the ones obtained for $C = 0$. In the fitting procedure the determining factor in finding C after all the other parameters are fixed is the shape of the envelope of fringes.

The method of data reduction for finding the magnitude of the cubic susceptibility $\chi^{(3)}$ of the thin film proceeds as follows. The amplitude of the pump wave is found from Maker fringes generated from a control bare substrate measured just before measurements are made on the film under consideration. This takes into account all effects related to the detection system response. Bare substrate data also permitted the substrate dispersion and thickness to be fine tuned at this stage. All the known parameters are then input into Eq. (5) along with guesses for C and $\chi_f^{(3)}$ until a good fit is obtained. Typical fits to a bare fused-silica substrate and two films with different magnitudes of $\chi^{(3)}$ are shown in Figs. 3(a), 3(b), and 3(c), respectively.

Table 2. Film Thicknesses, Refractive Indices, and Third-Order Nonlinear Susceptibilities $\chi^{(3)}(-3\omega;\omega,\omega,\omega)$ for Polysilanes and Polycarbosilanes

Polysilane	Film Thickness (nm) ±2%	n(1064 nm) ±2%	n(355 nm) ±10%	$\chi^{(3)}(-3\omega;\omega,\omega,\omega)$ (10^{-12} esu) ±20%
A	110	1.71	1.84	4.4
B	90	1.56	1.62	1.4
	596	1.56	1.63	0.75
C	227	1.74	1.84	1.2
D	87	1.75	1.88	3.4
	240	1.75	1.89	3.6
E	90	1.66	1.75	3.1
	462	1.66	1.77	1.6
F	227	1.61	1.63	0.34
G	198	1.67	1.69	0.37

RESULTS AND DISCUSSION

The $\chi^{(3)}$ values obtained from THG measurements on the series of polysilanes and polycarbosilanes are presented in Table 2. The uncertainties in these values are estimated to be ±20%, with the main contribution being the determination of the refractive index at 355 nm from the Kramers–Kronig fits. Clearly, poly(methylphenylsilane) (A) has the highest $\chi^{(3)}$ value (4.4×10^{-12} esu). This value is consistent with those obtained previously for films of this compound by Baumert *et al.* (7.2×10^{-12} esu),[12] Kajzar *et al.* (1.5×10^{-12} esu),[11] and Shukla *et al.* (6.8×10^{-12} esu).[14] The two polymers having the next highest $\chi^{(3)}$ values are compounds D and E, which also both have a phenyl substituent on the polysilane backbone. Enhanced values of $\chi^{(3)}$ for aryl-substituted polysilanes have previously been observed by Shukla *et al.*,[14] who found values in the range 4.9×10^{-12}–6.8×10^{-12} esu for polymers with phenyl as one side group, a factor of 2 or 3 larger than the values for comparable unsymmetric dialkyl polysilanes. The magnitude of $\chi^{(3)}$ for alkyl and aryl polysilanes is dependent on several factors. The electronic structure of the polymers, which is dependent on the substituents, is clearly a major factor, but nonlinear optical properties have also been shown to be dependent on backbone conformation as well as film thickness and orientation.[12,14,19] The electronic structure of substituted polysilanes has been investigated by Takeda *et al.*[20] Aryl substituents tend to increase delocalization of the σ and σ^* states, which are associated with the Si backbone, through mixing with the π and π^* states of the phenyl ring. Thus it may be expected that aryl-substituted polysilanes should exhibit enhanced $\chi^{(3)}$ coefficients compared with their alkyl-substituted counterparts. However, this delocalization results in a bathochromic shift of the σ–σ^* absorption band in aryl polysilanes, as can be seen from the data in Table 1. As the absorption band becomes shifted toward the third-harmonic frequency (for experiments carried out with the Nd:YAG fundamental at 1.064 μm), it becomes difficult to attribute enhancement of $\chi^{(3)}$ simply to electronic effects resulting from the change in substituents on the polysilane chain, since resonance effects will become increasingly important for those compounds having absorption bands close to 355 nm. It was previously suggested that the values of $\chi^{(3)}$ for aryl-substituted polysilanes determined at 1.064 μm are resonance enhanced owing to the proximity of the third-harmonic frequency to the absorption maximum of the polymer.[11,12,14]

There are other factors that may play a role in determining the relative magnitudes of the $\chi^{(3)}$ values presented in Table 2. The importance of polysilane conformation on optical properties was illustrated previously.[19,21,22] In particular, some symmetrical dialkylsilanes have been shown to undergo side chain crystallization, resulting in temperature-dependent optical properties.[12,22] As a result, poly(di-*n*-hexylsilane) has exhibited the largest $\chi^{(3)}$ coefficient measured to date for this class of materials.[12] The compounds studied here are all unsymmetrical and are expected to form random coil configurations in solution and amorphous thin films. The accepted model for the conformation of these compounds is that of a series of discrete *trans* backbone segments separated and partially electronically decoupled by one or more *gauche* or other nonplanar entities.[6,21,22] Since all the polysilanes in this study are similar in conformation and are noncrystalline, effects from conformational differences are likely to be small. It is possible, however, that differences in arrangements or lengths of *trans* segments may account for the differences in the $\chi^{(3)}$ values for copolymers D and E, compared with polymer A. For the two polycarbosilanes, F and G, with short Si–Si sequences interrupted by nonconjugated carbon links, it is clear from both the absorption maxima and the magnitude of the $\chi^{(3)}$ values that there is little effective conjugation length in these polymers. However, the $\chi^{(3)}$ values for the polycarbosilanes do exhibit some enhancement over the value for fused silica (a factor of ~12), and it may be possible to enhance this further by the use of conjugated carbon moieties to bridge the Si–Si backbone segments. Materials of this class may be promising for applications in nonlinear optics if they can be engineered to have optimal electronic and conformational properties.

The processing methods used to fabricate thin films of polymer may also have an effect on the magnitude of the nonlinear optical coefficients. Previously, the $\chi^{(3)}$ values for poly(methylphenylsilane) and poly(di-*n*-hexylsilane) were shown to depend on film thickness, with thinner films exhibiting higher $\chi^{(3)}$ values.[12] This has been attributed to orientational effects in thinner films. We observe a similar effect for some compounds, as illustrated by the data in Table 2 for compounds B and E. Other compounds produced films that gave $\chi^{(3)}$ values with no apparent dependence on film thickness in the range examined (80–600 nm). This is evident in the case of compound D. For this series of polymers the physical properties of the solutions vary quite substantially, and it is possible that different polymer molecular weight distributions and solution viscosities result in varying degrees of orientation in the films. We have also observed significant shifts in the λ_{max} values between the solutions used to form the films and the films themselves, indicating that processing is an important consideration. For example, the λ_{max} value for polysilane C in toluene is 304 nm, whereas a film spun from this solution exhibits a λ_{max} value of 321 nm. This is the largest shift observed, but other polysilanes also exhibit differences in absorption maxima between solution and films. The reason for these shifts is not clear but may originate in the orientation of the polymers in films produced by spinning. It is clear that processing techniques introduce some uncertainty into the determination of nonlinear optical coefficients for polymer materials in the form of thin films, and a fuller characterization of materials and films is desirable to facilitate comparisons of data from different laboratories.

CONCLUSIONS

Our results and those of others show that, while there are polysilanes that exhibit fairly high $\chi^{(3)}$ coefficients, the enhancement for those having the highest values can be attributed to resonance effects or to crystallization of the side chains leading to conformational changes. In general, alkyl and aryl polysilanes all exhibit $\chi^{(3)}$ values in the range 10^{-12}–10^{-11} esu, and, resonance and crystallization

effects aside, side group substitution alone seems unlikely to enhance the nonlinear optical properties of this class of materials much further. However, in general, polysilanes provide many interesting optical properties and offer extensive scope for engineering the structure and the properties. It is possible that further development in the areas of side chain substitution with moieties having distinct electronic properties and of orientation effects in polymer films by techniques such as Langmuir–Blodgett film deposition may yet yield materials with significantly enhanced nonlinear optical properties.

ACKNOWLEDGMENTS

Grateful thanks are extended to P. A. Hackett, National Research Council, for the loan of the Nd:YAG laser system.

C. A. Carere is a student in the Co-operative Education Program, University of Waterloo, Waterloo, Ontario N2L 3G1, Canada.

REFERENCES

1. J. Messier, F. Kajzar, P. Prasad, and D. Ulrich, eds., *Nonlinear Optical Effects in Organic Polymers,* Vol. 162 of NATO ASI Series E (Kluwer Academic, Boston, Mass., 1990).
2. P. N. Prasad and D. J. Williams, eds., *Introduction to Nonlinear Optical Effects in Molecules and Polymers* (Wiley, New York, 1990).
3. T. Tada and T. Ushirogouchi, "Si-containing electron resist materials for bilayer processing technology," Solid State Technol. **32**(6), 91–95 (1989).
4. D. C. Hofer, R. D. Miller, and C. G. Willson, "Polysilane bilayer UV lithography," in *Advances in Resist Technology I,* C. G. Willson, ed., Proc. Soc. Photo-Opt. Instrum. Eng. **469,** 16–23 (1984).
5. R. D. Miller, D. Hofer, G. N. Fickes, C. G. Willson, E. Marinero, P. Trefonas, and R. West, "Soluble polysilanes: an interesting new class of radiation sensitive materials," Polym. Eng. Sci. **26,** 1129–1134 (1986).
6. R. D. Miller, "Polysilanes—a new look at some old materials," Angew. Chem. Int. Ed. Engl. Adv. Mater. **28,** 1733–1740 (1989).
7. F. M. Schellenberg, R. L. Byer, and R. D. Miller, "Two-photon-induced birefringence in polysilanes," Chem. Phys. Lett. **166,** 331–339 (1990).
8. F. M. Schellenberg, R. L. Byer, R. D. Miller, and S. Kano, "Two-photon processes in substituted polysilanes," Mol. Cryst. Liq. Cryst. **183,** 197–210 (1990).
9. F. M. Schellenberg, R. L. Byer, and R. D. Miller, "Fabrication of birefringent gratings using nonlinear polysilane thin films," Opt. Lett. **15,** 242–244 (1990).
10. H. Nakano, Y. Ishida, T. Yanagawa, and N. Matsumoto, "Permanent grating induced by nonlinear absorption in polysilane films," Appl. Phys. Lett. **57,** 2876–2878 (1990).
11. F. Kajzar, J. Messier, and C. Rosilio, "Nonlinear optical properties of thin films of polysilane," J. Appl. Phys. **60,** 3040–3044 (1986).
12. J.-C. Baumert, G. C. Bjorklund, D. H. Jundt, M. C. Jurich, H. Looser, R. D. Miller, J. Rabolt, R. Sooriyakumaran, J. D. Swalen, and R. J. Twieg, "Temperature dependence of the third-order nonlinear optical susceptibilities in polysilanes and polygermanes," Appl. Phys. Lett. **53,** 1147–1149 (1988).
13. L. Yang, R. Dorsinville, Q. Z. Wang, W. K. Zou, P. P. Ho, N. L. Yang, R. R. Alfano, R. Zamboni, R. Danieli, G. Ruani, and C. Taliani, "Third-order optical nonlinearity in polycondensed thiophene-based polymers and polysilane polymers," J. Opt. Soc. Am. B **6,** 753–756 (1989).
14. P. Shukla, P. M. Cotts, R. D. Miller, S. Ducharme, R. Asthana, and J. Zavislan, "Nonlinear optical studies of polysilanes," Mol. Cryst. Liq. Cryst. **183,** 241–259 (1990).
15. D. S. Chemla and J. Zyss, eds., *Nonlinear Optical Properties of Organic Molecules and Crystals* (Academic, Orlando, Fla., 1987), Vol. 2.
16. S. Gauthier and D. J. Worsfold, "The effect of phase transfer catalysts on polysilane formation," Macromolecules **22,** 2213–2218 (1989).
17. F. Kajzar and J. Messier, "Third-harmonic generation in liquids," Phys. Rev. A **32,** 2352–2363 (1985).
18. J. W. Fleming, "Optical glasses," in *CRC Handbook of Laser Science and Technology,* M. J. Weber, ed. (CRC Press, Boca Raton, Fla., 1986), Vol. IV.
19. R. D. Miller and J. Michl, "Polysilane high polymers," Chem. Rev. **89,** 1359–1410 (1989).
20. K. Takeda, H. Teramae, and N. Matsumoto, "Electronic structure of chainlike polysilane," J. Am. Chem. Soc. **108,** 8186–8190 (1986).
21. R. D. Miller, J. F. Rabolt, R. Sooriyakumaran, W. Fleming, G. N. Fickes, B. L. Farmer, and H. Kuzmany, Chap. 4 of *Inorganic and Organometallic Polymers,* M. Zeldin, K. J. Wynne, and H. R. Allcock, eds., Vol. 360 of ACS Symposium Series (American Chemical Society, Washington, D.C., 1988).
22. J. Michl, J. W. Downing, T. Karatsu, K. A. Klingensmith, G. M. Wallraff, and R. D. Miller, Chap. 5 of *Inorganic and Organometallic Polymers,* M. Zeldin, K. J. Wynne, and H. R. Allcock, eds., Vol. 360 of ACS Symposium Series (American Chemical Society, Washington, D.C., 1988).